
4 Image Analysis of plastic deformation in the fracture of paper

4.1 Introduction

As detailed in Chapter 2, one of the fundamental problems that arises in the estimation of the fracture toughness of an elastic-plastic material like paper is the significant amount of plastic deformation that can occur in areas away from the Fracture Process Zone (FPZ). A brief summary of the mechanism that leads to the plastic deformation is given here.

When a tough, non-linear elastic-plastic material with a crack is strained, the material will offer resistance against the crack propagation. The resistance offered by the material against crack propagation is the fracture toughness. When large loads are applied to the material, it can yield not only in the area just ahead of the crack-tip (the Fracture Process Zone (FPZ)), but in areas away from the FPZ as well. In such circumstances the work that is consumed for plastic deformation in areas away from the FPZ is not a part of the fracture toughness, and hence needs to be excluded from the total work. The EWF technique is a method of separating the work in the FPZ from the work of plastic deformation. However, the EWF technique requires measurements of a large number of samples at many different ligament lengths in order to perform this separation. There is no direct or easily applicable method that can be used to estimate the work consumed in the outer plastic zone.

The original aim of using an image analysis technique was to obtain more information on the outer plastic region and also to see whether this information can be used to quantitatively estimate the work consumed for plastic deformation. If the work spent for the plastic deformation in the outer plastic zone can be successfully independently estimated, then the fracture toughness of the material can be obtained by subtracting this plastic work from the total work obtained from a single ligament DENT sample. This could significantly reduce the amount of time required for multiple ligament sample preparation, testing and analysis in the EWF or J-integral methods. Another advantage

would be that testing at a single ligament length would use much less sheet area than that generally required for a full EWF test. The other possible importance of the image analysis technique is that additional information could be acquired from this technique, such as the shape and extent of the outer deformation zone, which can be used to test the validity of the assumptions behind the EWF technique. Some of the pre-conditions of using the EWF technique are that: (a) the DENT specimen should yield completely before fracture (b) the deformation field around the ligament should have formed a uniform shape before fracture commences and (c) the plastic deformation work should scale with the ligament length squared.

4.2 Samples, apparatus and the technique

The samples used in this experiment were 80 g/m² “Reflex” copy paper manufactured by PaperlinX. A software package (Corel Draw 7.0) was used to design fine lines (250 μm apart) that were printed on the sample along the Machine Direction (MD) or the Cross machine Direction (CD) according to requirements.

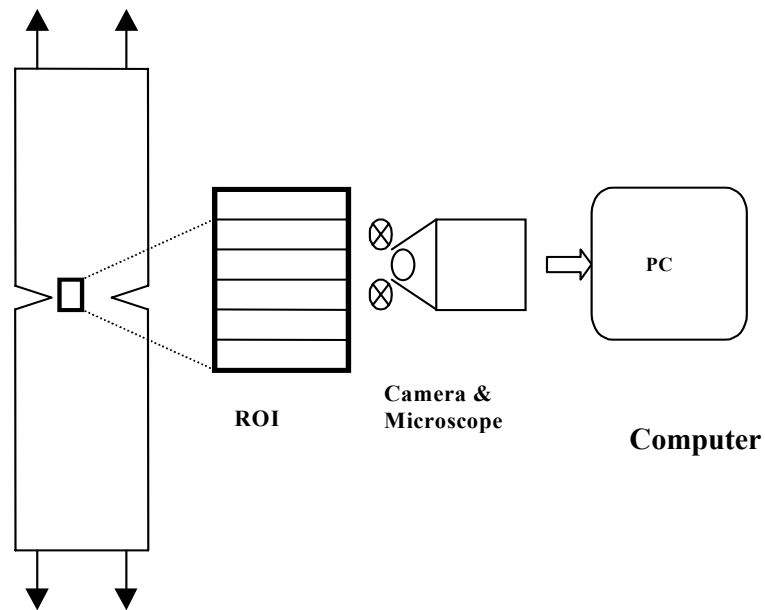


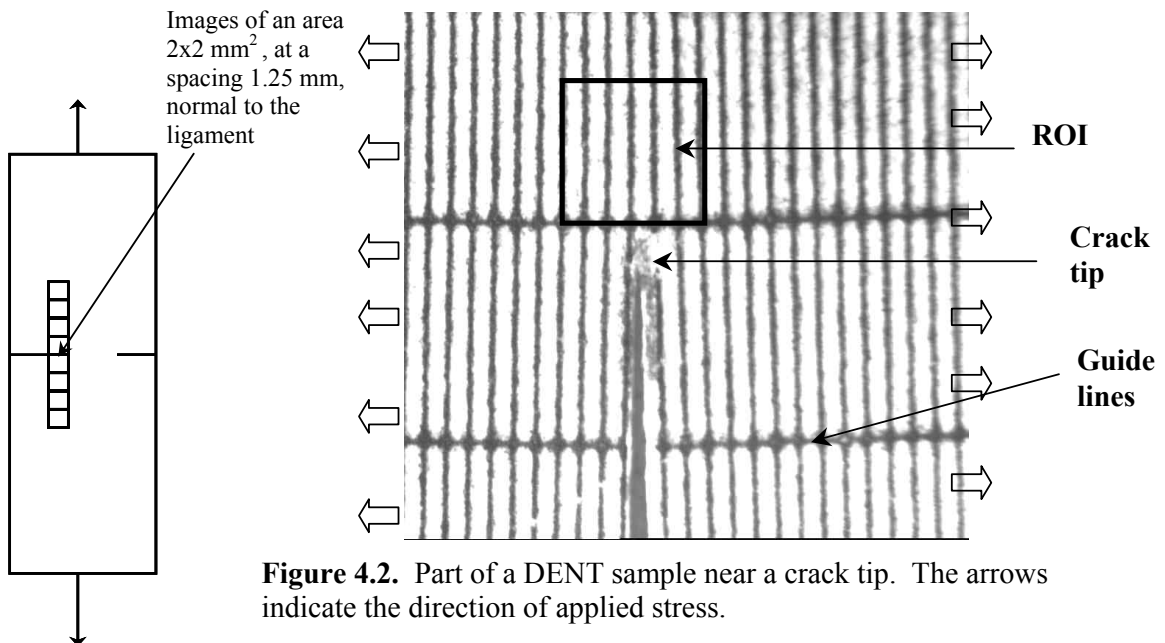
Figure 4.1 Experimental set-up for image capturing system

The image analysis technique essentially estimates the distance between fine printed lines (at a given position) from images captured before and after straining the sample. The distances were each an average of the distances between seven or eight lines in one

given image. Comparing the same image before and after straining allows the average strain to be estimated.

Figure 4.1 shows the experimental set up used for the image analysis. Images of a Region Of Interest (ROI) were captured using an OLYMPUS SZ40 microscope, a PULNiX TM-6CN CCD camera and a personal computer equipped with a MACH Series DT 3155 frame capture card, before and after straining in the Instron. The guidelines (see Figure 4.2) printed perpendicular to the fine lines were used to locate exact positions in the test pieces during image capture. It was necessary to remove the sample from the Instron to capture the images. This is because it is necessary to move the sample under the microscope in order to capture the series of images required to measure the whole deformation field. This was not possible while the sample was mounted vertically in the Instron.

A fundamental assumption of the EWF technique is that the outer plastic zone is circular or elliptical with diameter L . The ligament length L , of the DENT sample used in this experiment was 15 mm. To test the validity of this assumption, images were collected over an area that was larger than the expected size of the deformation zone.



To accomplish this task a series of images, at a spacing of 1.25mm, were captured along a 25mm line, normal to and centred on the ligament (see the left insert in Figure 4.2). The microscope magnification was set to capture images containing 7 or 8 lines (in an area of about $2 \times 2 \text{ mm}^2$) so that the average line spacing could be obtained accurately.

Figure 4.2 illustrates a ROI near the crack tip of a sample. A typical captured image is shown in Figure 4.3. Optimas image-processing software was used to obtain an average gray scale value for each one pixel wide column, which was set perpendicular to the direction of the applied stress, and the whole image was converted to an intensity profile. Minima in the transformed profile represent the centres of the dark lines, where the gray-scale intensity is a minimum. The gray scale values were then inverted by subtracting them from the maximum gray scale value of 255 to convert the dark lines from valleys to peaks. The resulting data were exported as a text file. The centres of the peaks were obtained using a peak-fitting program “Peaksolve”. Figure 4.4 shows a typical inverted gray scale plot obtained after processing the image in Figure 4.3, together with the fitted curve obtained from the peak-fitting program. It can be seen that the peak fits obtained were good and that the accuracy of the estimated peak centers was within ± 0.03 pixel. Averaging 7 or 8 peak centres further reduced the uncertainty of these values. Finally, with the aid of spreadsheet software, the average line spacing and its uncertainties were obtained from a fit of the peak positions.

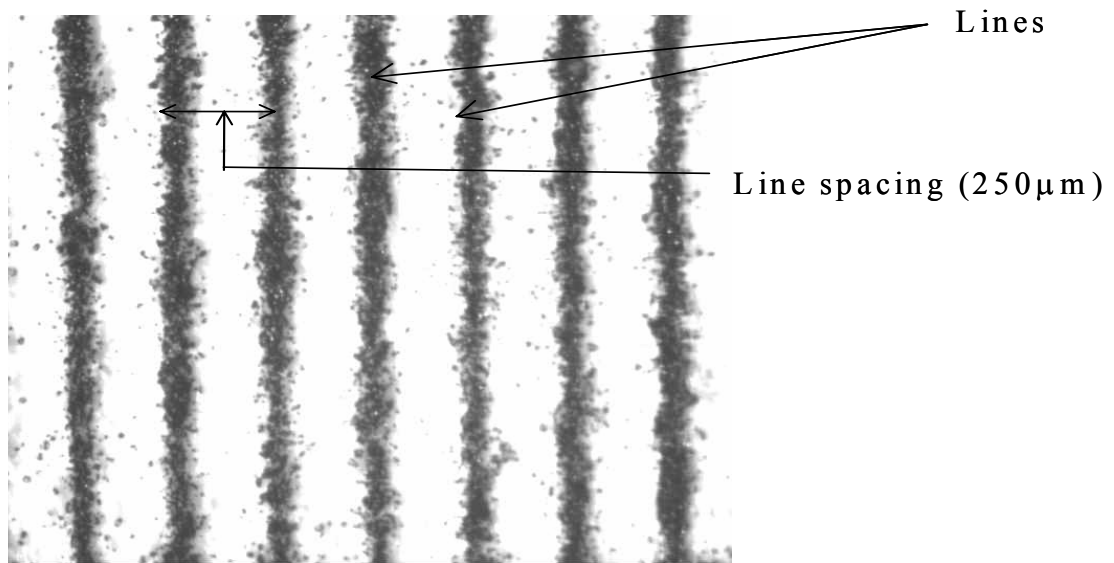


Figure 4.3. A typical image showing 7 lines. (Lines are $250 \mu\text{m}$ apart)

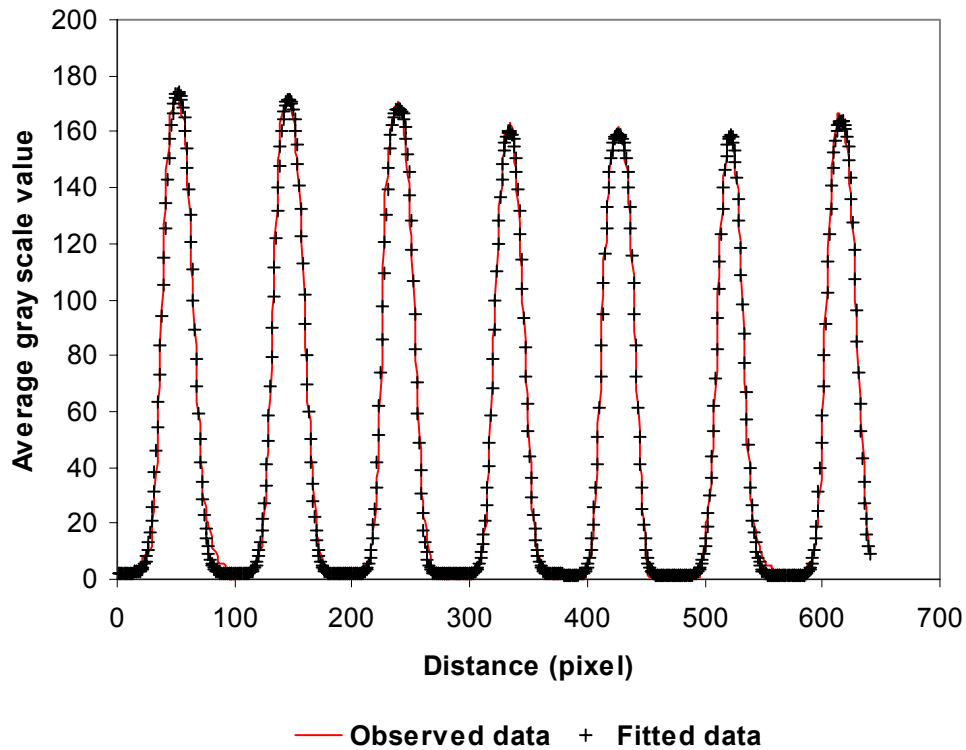


Figure 4.4. Inverted average gray scale plot for the image in Figure 4.3 (the crosses give the fitted curve)

4.3 Sample straining

The samples were strained using the grips for EWF testing described in Chapter 3. The cross-head speed of the Instron was set at 0.5 mm/minute. The vertical guide-rods were used in the rig during these tests to ensure that the sample is loaded in-plane. The friction due to guide rods was subtracted from the area under the load elongation curve during the analysis. The average breaking load of the sample was obtained by testing 12 test pieces and this value was used as a guide to decide when to terminate the straining process. A microscope was also used to observe the notch tip and to determine the critical point to stop straining before the crack began to propagate.

4.4 Calibration

To check the accuracy of the technique for determining strain, real-time images from the middle of a printed tensile test piece with 100 mm span were captured at a rate of 1.8 frames/second. The sample was commercial copy paper, strained in the CD direction at a strain rate of 0.5 mm/min (0.0083% per sec.). The lines were printed

normal to the applied stress. A comparison was obtained between the set linear strain rate (0.0083% per sec.) and the experimental strain rate determined by image analysis.

Figure 4.5 shows the results obtained from the CD tensile test piece. The line spacing variation in this localised region was well fitted with a linear relationship, indicating a constant strain rate. The peak fitting procedure to find peak centres and the procedure of averaging 7 to 8 line spacings has significantly improved the accuracy of the obtained values compared to measuring only a single line spacing. It can be seen from Figure 4.5 that this technique is highly sensitive and the average change in line spacing between frames was 0.0052 ± 0.0003 pixels. The error was estimated from 95% confidence intervals. The strain rate was determined from the slope of the linear fit divided by the y-intercept of the fit. The measured strain rate was $0.0091\% \pm 0.0003\%$ per second compared with the set strain rate of 0.0083% per second. There is thus a small difference between the experimentally measured and set strain rates. However, considering the fact that the paper is a less uniform material (i.e. local and global strain rates can differ), these results can be considered as within expectations. The most significant feature is the resolution of the technique, which is better than 0.01 pixels ($0.03 \mu\text{m}$) as can be seen from Figure 4.5.

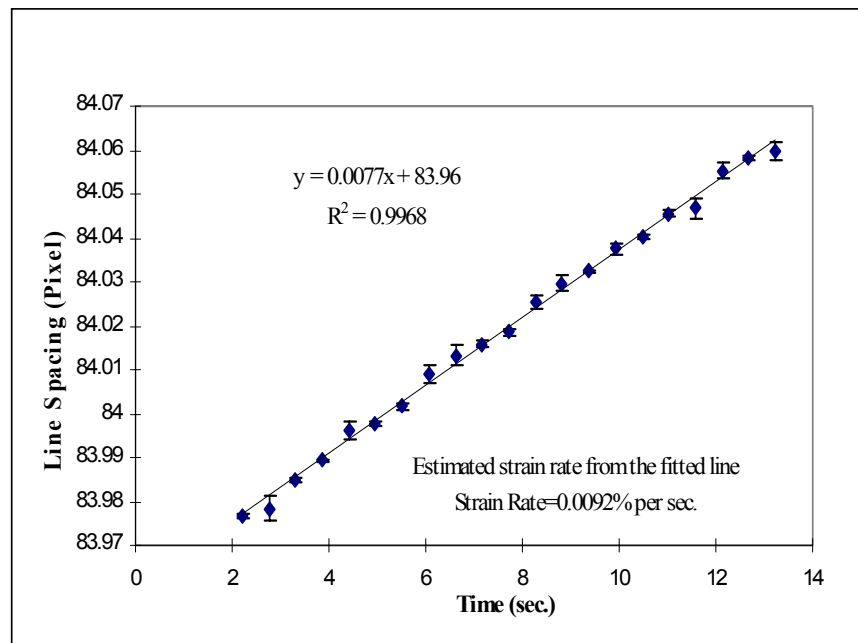


Figure 4.5 Line-spacing variation of a CD tensile test piece of copy paper with time

4.5 Plastic deformation measurements

This section presents the main measurements. First the critical load-elongation curves for the MD and CD tests are presented. These were used to determine how much to strain each sample.

4.5.1 Critical loads and displacements for DENT samples

In order to establish the load–elongation behaviour of DENT specimen under tensile load, 10 test pieces from both MD and CD direction were tested and average curves were obtained. The average load-elongation curves in CD and MD directions are showed in Figure 4.6. For the CD test, the first part of the load-elongation curve is linear (up to about 0.10 mm extension) indicating an elastic type straining. The deviation from linearity in the latter part of the curve is indicative of elastic–plastic behaviour. For the loading in the CD direction, the critical load and extension obtained just before the crack began to propagate were about 33 N and 0.5 mm respectively. For loading in the MD direction, the critical load just before crack extension was approximately 53 N and the extension was about 0.42 mm.

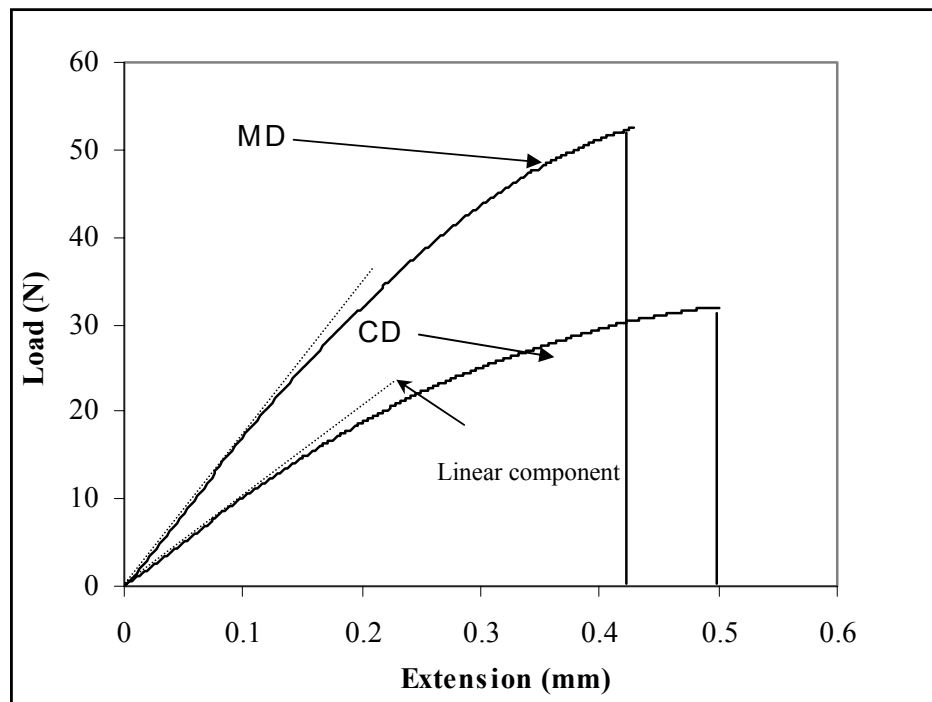


Figure 4.6. The average Load against Extension data for copy paper in the CD and MD direction for DENT test pieces. In both instances straining was stopped before crack propagation

Once the critical loads were established, the fine line printed DENT tests pieces were strained at a constant rate (2mm/min) until they reached the critical load. Real-time images of an area close to the crack-tip were captured while sample was straining (an area similar to that shown in Figure 4.2 as the ROI). The line spacing variation or strain of this region was compared with the set strain rate.

The span of the DENT test piece tested was 100 mm. A non-linear change in line spacing with time is clearly evident in the DENT test piece subjected to constant rate of elongation (see Figure 4.7). This behaviour is a result of high stress concentration at the crack-tip compared to the stress distribution in other areas of the test piece. In this case the comparison of estimated strain rate from image analysis with the set strain rate was meaningless, since the straining at the crack tip was significantly larger and also non-linear compared to the set strain rate.

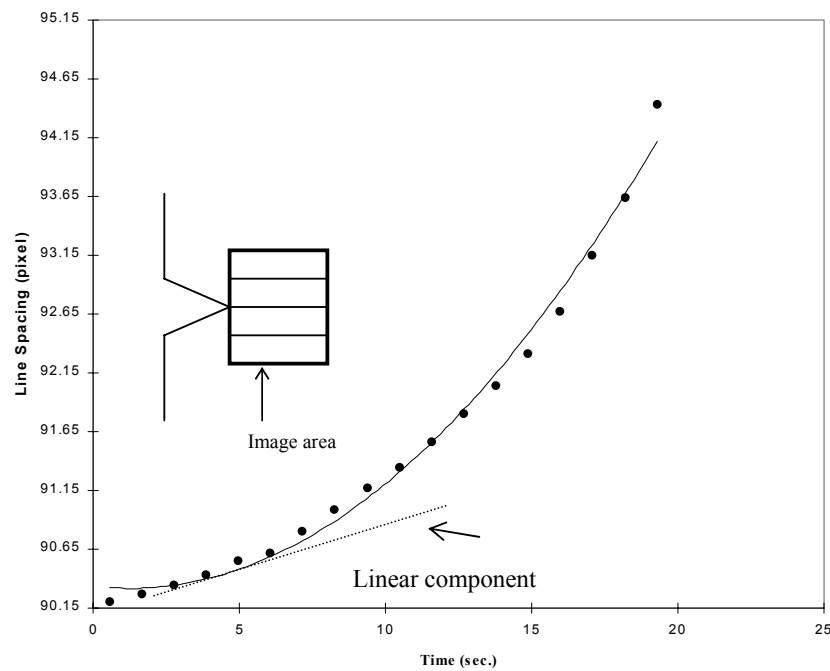


Figure 4.7. Line-spacing variation of DENT sample near the crack-tip. “Reflex” copy paper in CD direction

The next sections give the plastic deformation fields measured from the images captured from the CD and MD DENT test pieces, normal to the ligament, before and after the test pieces were strained.

4.5.2 CD DENT test piece

Figure 4.8 shows the variation in the average line spacing, in pixels, for each image captured along the first guideline in the CD direction. The x-axis gives the distance from the ligament to the centre point of the image. One data set (filled circles) shown in this figure was obtained from images captured before straining the test piece.

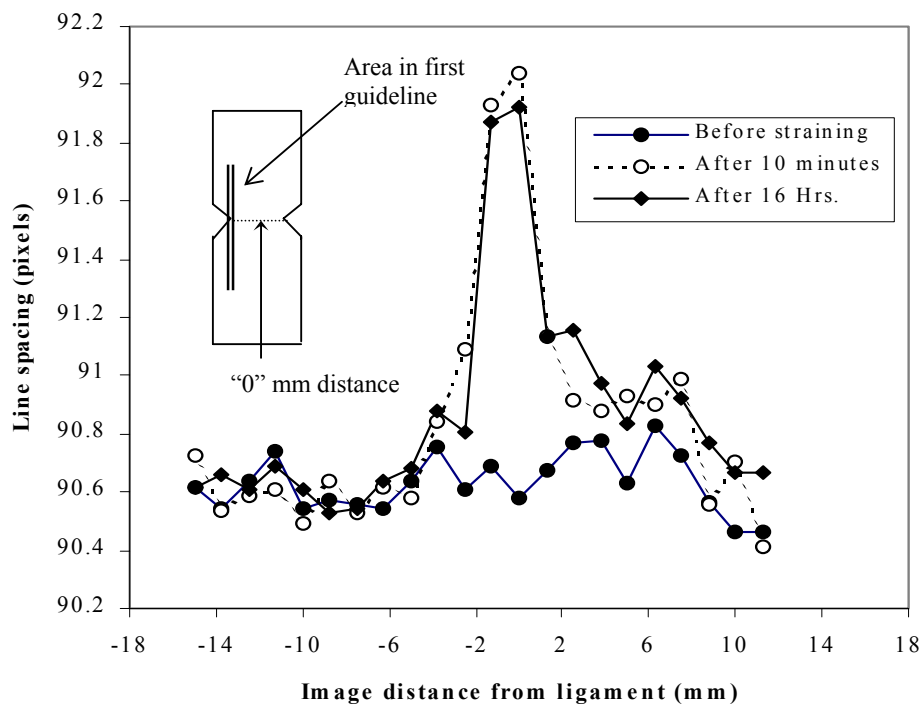


Figure 4.8. Variation of line spacing with image distance (from the ligament, along 1st guideline) for copy paper strained in the CD direction.

A second set (open circles) was obtained from images captured soon after straining. (Although image capturing was started soon after the straining, it takes about 10 to 15 minutes to complete image capture along one guideline.) A third set (filled diamonds) was obtained from the images captured after leaving the test piece at 23°C and 50% RH for nearly 16 hours after straining. This was done to examine whether there was any relaxation of the plastic strain over longer periods of time.

Although there is a reduction in the line spacing of the image located close to the middle of the ligament (0 mm distance) of the sample left for 16 hours, compared to that of sample left for 10 minutes, it is difficult to assume that this reduction was due to relaxation of the plastic strain, as this difference is most likely due to errors. This is because, while the line spacing of an individual image can be determined to better than 0.01 pixel precision, it was not possible to align the sample under the microscope to capture exactly the same area each time.

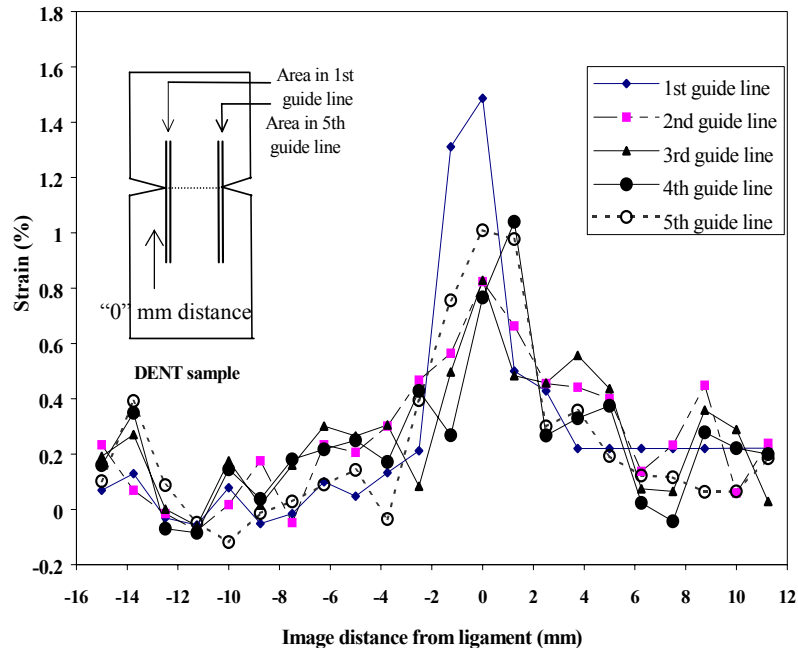


Figure 4.9. Strain (%) versus frame distance from ligament along each guideline for copy paper in CD after straining. These data were taken after 16 hours of conditioning

The maximum change in line spacing due to straining of the sample was about 1.4 pixels. This is equal to a plastic strain of 1.5 %. Figure 4.9 shows the irreversible plastic strain (%) as a function of position along the 5 guidelines normal to the ligament length. The distance from the middle of each frame to the ligament was taken as the position of the frame. The data in Figure 4.9 show that the position of maximum strain along each guideline was on the ligament ($x=0$) except for the data obtained along the 4th guideline, where the position of maximum strain was located 1.25 mm away from the ligament position.

The strain plots in Figure 4.9 indicate that the effective deformation field estimated along guidelines 2 to 4 in the sample extended a distance of about 5mm on both sides of

the ligament. Although consistency is expected, some variation in strain is apparent in the images taken from the same distance from the ligament, along different guidelines, well away from the notch-tips. This can be seen in the way the apparent plastic strain at positions well away from the ligament varies from 0.4 % to 0.1 %. One reason for such behaviour could be due to variations in local strain fields, which can occur in a non-uniform material like paper. Another reason could be due to some variations in image location from measurement to measurement. After capture of the initial images, the test pieces were moved from the image capturing stage to the straining rig and taken back to the stage for capture of images after straining. This process introduces errors in locating the same localised position in the test piece, even though the guidelines were used. The appearance of negative strains is likely to be a consequence of such differences in the image positions when capturing images before and after straining the sample.

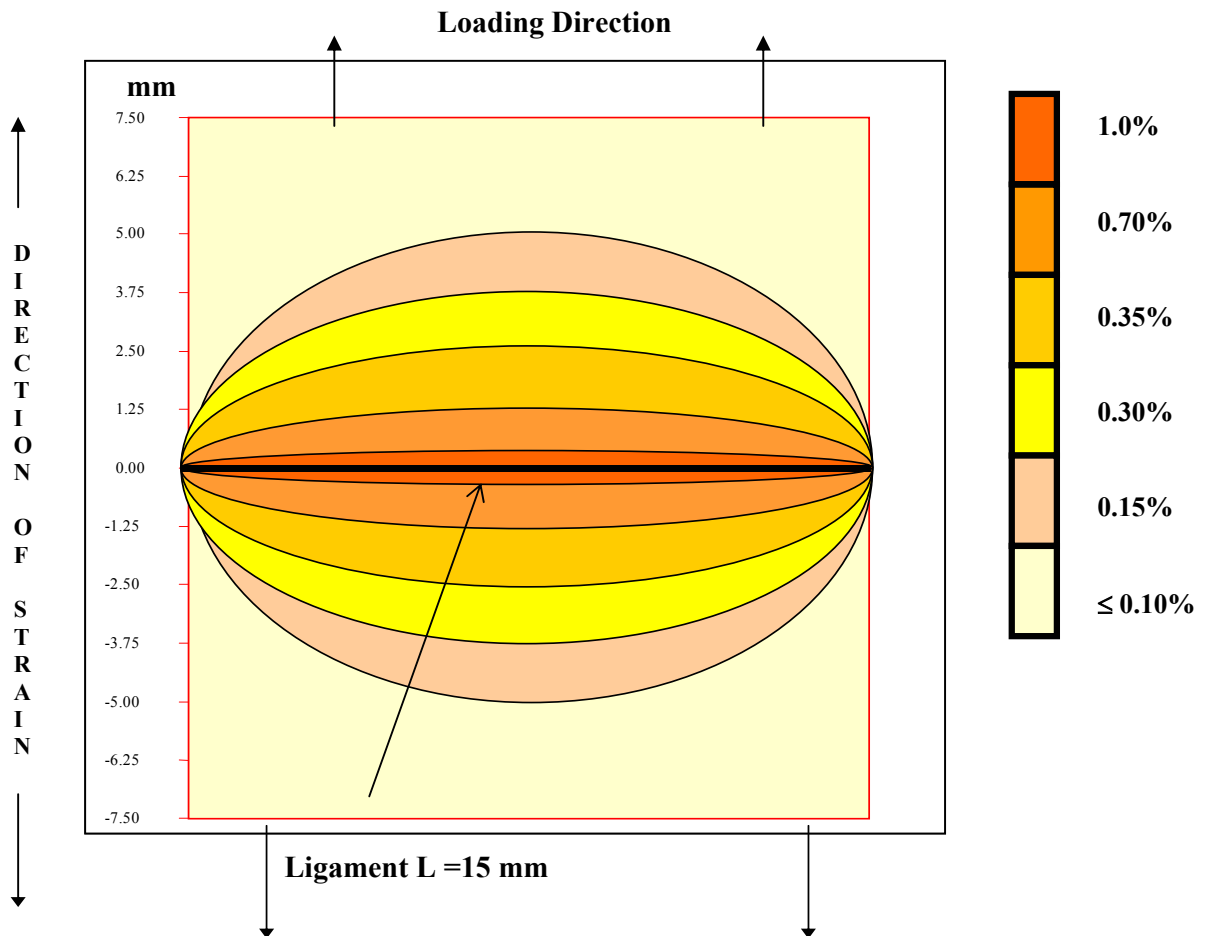


Figure 4.10. Illustration of strain profile around ligament of Reflex copy paper in CD direction

Figure 4.10 illustrates schematically the strain profile around the ligament in CD direction. This was drawn to obtain an idea about the extension of the strain field. The y-axis (in mm) is the distance from the ligament of the DENT sample to locations parallel to the ligament. Different gray scale values represent various magnitudes in strain fields. These values were obtained by averaging the strains from the same position on either side of the ligament.

Although this is not a comprehensive illustration, this strain profile provides some useful information about the spreading of the strain field and its shape. The areas with strains $\leq 0.1\%$ are areas where no plastic strain observed. Figure 4.10 shows that the average strain (%) along the ligament (0mm distance) was 1.0%. The effective strain field has extended only a distance of 5 mm from either side of the ligament. The sharp peaks near the crack tips (as in Figure 4.9) and the 5mm extension of the effective plastic strain fields suggest that the overall strain distributions along the guidelines is more elliptical than circular. This observed strain field is not in full agreement with the assumption of the EWF technique.

4.5.3 MD DENT test piece

The line spacing in the MD test piece, showed considerable variation along the guidelines even before the sample was strained (see Figure 4.11).

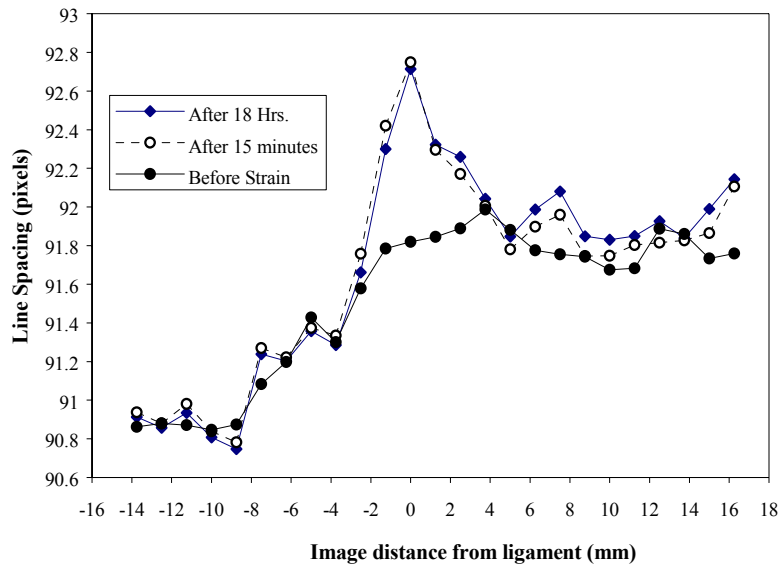


Figure 4.11. Line-spacing variation with image distance (from ligament), along 1st guideline for testing in the MD direction

This seems to be a result of the way the sample was loaded into the printer. This variation was more severe when paper was fed in the MD direction to the printer. To reduce the variation, the graphic design (fine line) generated in the computer was rotated by 90° , and printed on a test piece that was fed in the CD direction to the printer. After straining, the highest magnitude of plastic strain occurs at the ligament.

The strain variation along the first three guidelines from one of the crack tips is shown in Figure 4.12. It is quite significant that no plastic strain along the second and third guidelines can be measured. This indicates that the deformation field is located only around the notches and does not extend over the whole ligament. This compares with the strain field in the CD test piece, which was approximately elliptical in shape and extended over the whole ligament length. These observations suggest that MD DENT sample with ligament $L=15$ mm has not fully yielded before the crack begins to propagate. This violates one of the central conditions of the EWF method.

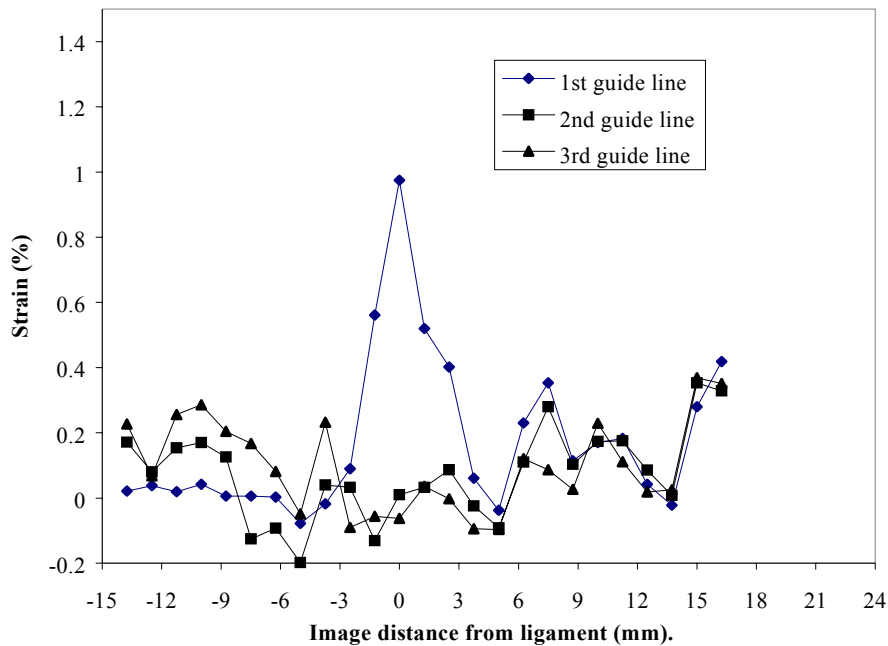


Figure 4.12. Strain (%) versus image distance (from ligament) obtained along three guidelines for copy paper in MD after straining. These data were taken after 18 hours conditioning

4.6 Estimation of plastic work in “Reflex” copy paper (CD direction)

The strain profile of the outer plastic zone obtained from the image analysis technique was used to estimate the plastic work in the outer plastic zone of the DENT sample when tested in the CD direction. The steps in the calculations were as follows:

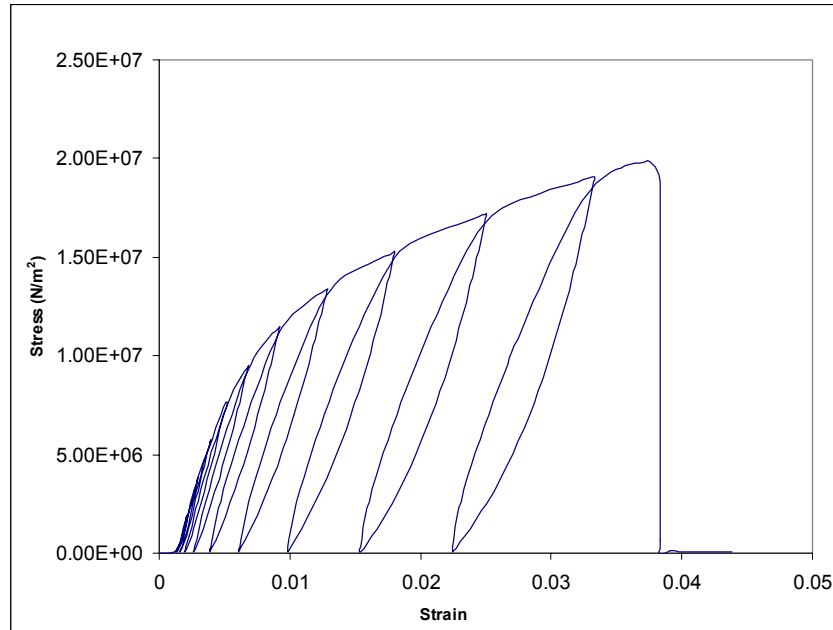


Figure 4.13. Stress versus strain of cyclically loaded tensile test piece of “Reflex” copy paper tested in the CD direction.

The first step was to estimate the work required to apply a given plastic strain to a unit area of the material. The first step in doing was to cyclically load a tensile test piece of “Reflex” copy paper in CD direction, and the maximum load in each cycle was increased from cycle to cycle in 1N increments, to obtain a load-extension curve. The strain rate was set to 2 mm /minute, which was the rate used for straining the DENT test pieces. The sample width was kept at $L=15\text{mm}$ which was equivalent to the ligament L of the DENT sample. Also the sample length was kept similar to that of DENT sample. Figure 4.13 shows the results of this cyclic loading procedure.

The cyclically loaded stress – strain curve enables a relationship between plastic work per unit volume or “specific plastic work” and plastic strain to be constructed. There is no plastic work until the strain exceeds the elastic limit of the test piece. Thus the first data point was taken as the origin since there is no plastic work at zero plastic strain.

The second coordinate was obtained by relating the work in the first cycle with the corresponding plastic strain at the end of the first cycle. Estimating the work under the envelope of the first two cycles and relating it with the plastic strain resulting after two cycles gave the third data point. The other points were obtained by following the same procedure for each subsequent cycle.

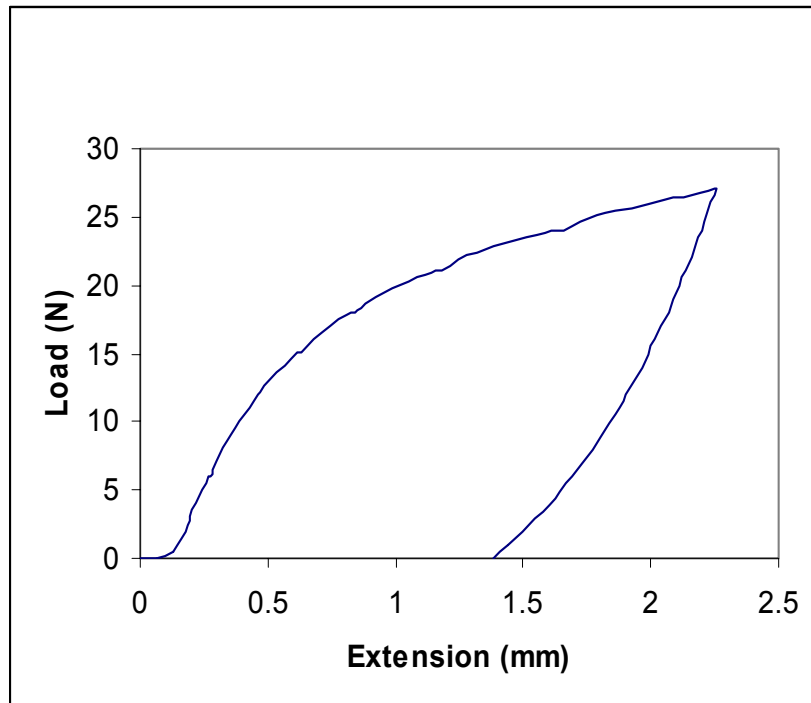


Figure 4.14. Envelop of nine cycles of the load-extension curve of cyclically loaded “Reflex” copy paper CD direction tensile test piece.

An example of the application of the technique is shown in Figure 4.14, which shows the envelop of nine cycles of the cyclically loaded load-extension curve. The total work under the curve was calculated to be 63.5×10^{-3} J, which corresponded to a plastic strain of 1.46%. The specific plastic work was obtained by dividing the total work from the sample volume 1.42×10^{-7} m³ (90mm x 15mm x 0.105 mm). Once the data were obtained, a graph was plotted between specific plastic work and plastic strain (%) for “Reflex” copy paper, as shown in Figure 4.15. A polynomial that passes through the origin was fitted to the data from which the relationship $y = -4.3 \times 10^4 x^3 + 1.9 \times 10^5 x^2 + 1.3 \times 10^5 x$ was obtained, where x is the plastic strain (%) and y is the specific plastic work. The correlation coefficient of this fitting was $R^2 = 0.9991$ and hence the use of this equation to relate plastic strain and specific plastic work was quite reasonable.

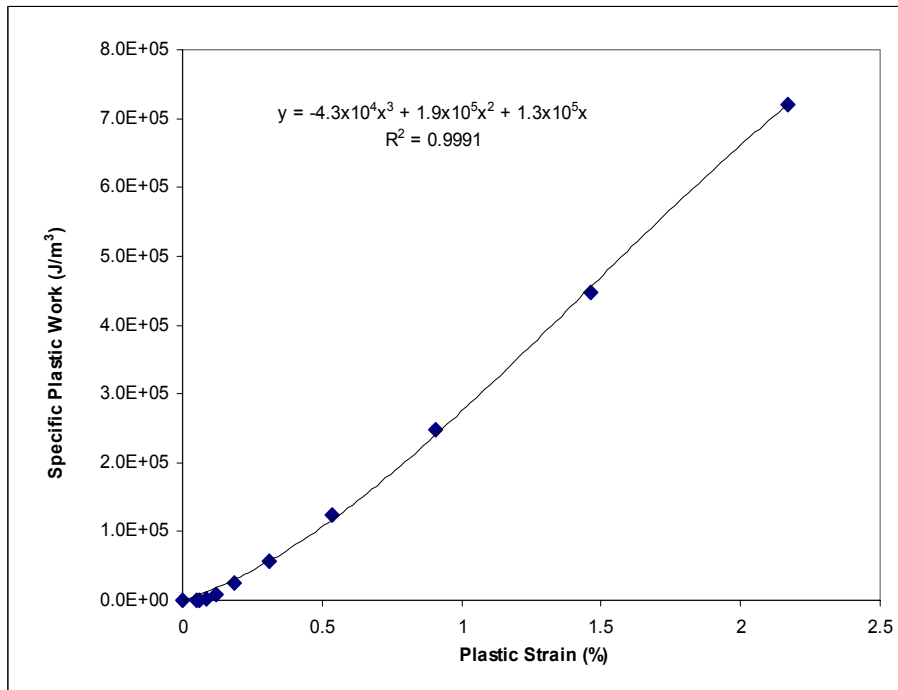


Figure 4.15. Plastic strain (%) versus specific plastic work for “Reflex” copy paper tested in the CD direction.

This equation was used to convert plastic strain (%) of each ROI represented by individual points in the graph of Figure 4.9 to specific plastic work. The total specific plastic work in a given guideline was obtained by adding the individual specific plastic work of each ROI. The grand total of specific plastic work in the whole plastic zone was then obtained by adding the specific plastic work from each guideline.

Figure 4.16 shows the variation in specific plastic work along the guidelines of “Reflex” copy paper in CD direction. A high consumption of specific plastic work can be seen close to the left notch of the DENT sample, and a gradual decrease in the plastic work when moving towards the middle of the sample can also be observed. A slight increase of plastic work can be seen at the 5th guideline, which is close to right crack tip. As the width of the guidelines was greater (3mm) than the width of the ROI, plastic work was calculated by taking this area within the guidelines into account. The spacing between images was 1.25mm and it was assumed that estimated plastic strain in an image was applicable to an area 1.25mm x 3.00mm. Hence the volume was calculated by $L \times W \times t$, where L and W are the length and width of the guideline, respectively and t is the

thickness of the sample and the volume was $3.94 \times 10^{-10} \text{ m}^3$. The total plastic work was obtained by multiplying the specific plastic work by the estimated volume.

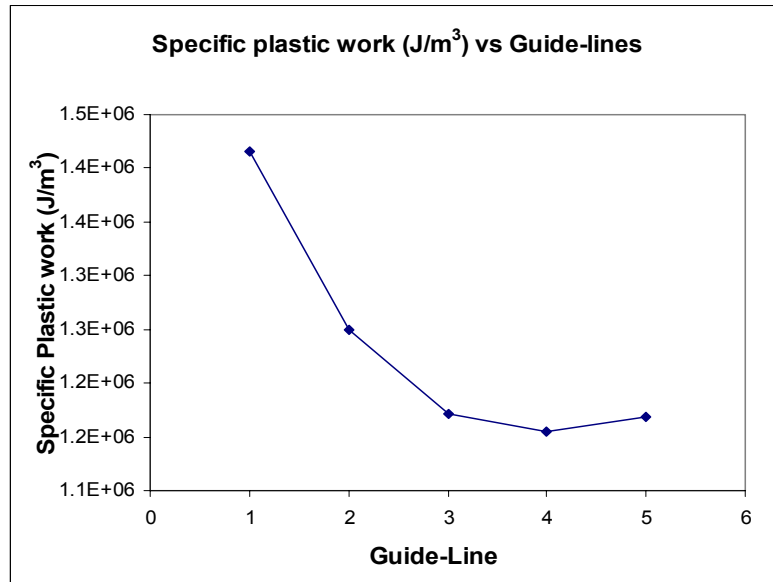


Figure 4.16. Variation of total average plastic work per unit volume along guidelines in “Reflex” copy paper (CD).

The calculated total plastic work in the outer plastic region was $2.4 \times 10^{-3} \text{ J}$ and this is about 12 % of the work under a load extension curve of a L=15mm DENT “Reflex” CD sample. The fracture toughness measurements carried out using a new cyclic technique (details of the technique is given in Chapter 6) has shown that the plastic work of “Reflex” copy paper in the CD direction is about 34% of the total work for a ligament length of L= 15 mm. Therefore image analysis plastic work calculation seems to underestimate the actual plastic work in the outer plastic zone. The reasons for this are discussed in the next section.

4.7 Discussion

This image analysis technique has shown a great deal of sensitivity in resolving changes in line-spacing as small as in $0.03\mu\text{m}$. However, some non-uniformity in fine lines printed on the sample surface and the difficulty in re-positioning the sample after straining to capture exactly the same area, decreased the resolution to around 0.1-0.2 pixels.

The marked difference in the plastic strain profile of CD direction and MD direction provides some useful information on yielding in the ligament area prior to the failure. For the CD direction an increased strain can be seen on the line across the ligament along all five guidelines indicating higher straining of the sample in this area compared to the area away from the ligament. On the other hand, a similar behaviour can be seen in the MD direction only along the guidelines next to the notches of the DENT sample. The strain profiles along the guide-lines away from the notches showed no significant plastic strain. This behaviour suggests that the CD direction DENT sample (with a $L=15$ mm ligament length) had fully yielded by the time the straining was stopped just prior to the crack propagation but MD direction sample hadn't. One of the fundamental requirements of using the EWF technique in measuring fracture toughness is that the ligament should completely yield before crack propagation. Therefore, these results suggests that if the EWF technique is to be used to measure fracture toughness of "Reflex" copy paper in the MD direction, the ligament length of $L=15$ mm cannot be used.

Tanaka *et al* (1997) used thermography measurements to classify the developing pattern of a DENT geometry sample's plastic deformation zone into three categories. A deformation field that appears whole through the ligament in an indistinct and speckled manner and developed into a circular or oval zone was classified as type I. Type II was defined as a deformation field that appears from the notch tips and amalgamates into a circular or oval zone after the point of maximum load. A deformation field that appears from the notch tips and that does not amalgamate to form a uniform deformation field was categorised as type III. According to these classifications the CD sample with $L=15$ mm is showing a type I deformation pattern since the strain profiles in Figures 4.9 and 4.10 clearly shows a formation of a uniform deformation field prior to crack propagation. On the other hand the deformation pattern in the MD direction seems to be of type II or III as no plastic deformation in the middle of the ligament can be observed. Since the straining was stopped prior to the crack propagation, it is difficult to say whether the deformation fields that formed around the notch tips would amalgamate or not to form a uniform deformation zone after the sample has began to fail. Tanaka *et al* (Tanaka 1998) further asserted that for many kind of papers there were two different slopes on a EWF plot for type I group and type II and III groups. The fracture toughness

w_e estimated from type I specimens is considered to give the true property of the material, provided that the tests satisfy the other assumptions in EWF method.

In a separate set of experiments the fracture toughness of “Reflex” copy paper in CD and MD direction was estimated using the EWF method (see chapter 5). The w_f (specific fracture energy) against ligament length (L) plot for “Reflex” copy paper tested in the CD direction (see Figure 5.2b) could be fitted by a single linear regression for the data points obtained for all ligament lengths up to $L=15$ mm. This confirms that Reflex copy paper tested in the CD direction with $L=15$ mm sample belongs to the type I category.

The EWF plot for “Reflex” copy paper MD shows two distinct linear trends to the data points obtained for ligament lengths of 6 mm or more (Figure 5.2a). The first linear regression extends up to the points with $L=9$ mm and the second linear regression, with lower slope, covers the rest of the points including $L=15$ mm. This behaviour suggests that the samples with $L \geq 10$ mm are displaying type II or III plastic deformation fields, which is completely consistent with the image analysis results presented in this chapter. Samples displaying either of these types of deformation fields have not fully yielded before failure has commenced, which violates one of the prerequisites for a successful measurement with the EWF technique. A linear regression fit to the $L \geq 10$ mm data produced a higher intercept than for the $6 \leq L \leq 9$ mm data, confirming that a type II or III deformation field will yield an erroneous result.

With regards to the plastic work calculations using strain profiles obtained for testing the copy paper in the CD direction, the cyclic fracture toughness estimates shows that the plastic work in CD direction for a sample with $L=15$ mm was about 7.4×10^{-3} J. This is approximately 3 times greater than the estimate from image analysis work presented here of 2.4×10^{-3} J. One main reason for such discrepancy could be the stopping of sample straining well before crack propagation. Although the point where straining was stopped was decided by observing the crack-tip through a microscope, a significant amount of error could be contributed from the selection of the point to stop straining. In addition, as the increase in plastic work is almost linear at this point (especially around crack tip), stopping straining prematurely may miss a large proportion of plastic work that actually occurs when the sample is strained until the

crack begins to propagate and hence this will lead to an underestimation of the plastic work.

4.8 CONCLUSIONS

This study shows that this new imaging technique can be used to characterise the deformation fields in paper. This technique can be used to measure strains of less than 0.1% in this system. The plastic deformation field in the CD test piece was found to be approximately elliptical. The deformation field in the MD test piece had not formed as a single field in the ligament, by the time straining was stopped. Therefore, for the copy paper tested in the MD direction, the ligament length $L=15\text{mm}$ is not suitable for the use in the EWF method.

The estimated plastic work in the CD direction was about 2.4×10^{-3} J and this was about 12% of the total work. However the expected plastic work was around 7.4×10^{-3} J. The premature stopping of sample straining seems to underestimate the actual plastic work that would have occurred if the sample had been strained until destruction.

These findings suggest that the image analysis technique can be used to study the deformation field of a DENT paper sample, but it cannot be used to accurately separate out the plastic work from the total work and thus allow the EWF fracture toughness to be measured from data at a single ligament length only. The image analysis technique simply takes too much time and is too inaccurate to consider using this method to speed up the EWF measurements. One further problem is that the image analysis measurements would have had to be done for each new sample type. This is because as will be shown in Chapter 5, there is only a poor correlation between fracture toughness and plastic deformation.